LAMINATE DESIGN WITH NON-STANDARD PLY ANGLES FOR OPTIMISED IN-PLANE PERFORMANCE

Mark W.D. Nielsen[1], Kevin J. Johnson[1], Andrew T. Rhead[1] and Richard Butler[1]

[1] MAST Research Centre, Department of Mechanical Engineering, University of Bath, Bath, UK, email: R.Butler@bath.ac.uk, web page: http://www.bath.ac.uk/mech-eng/

Keywords: Elastic energy, Minimum mass, Optimization, Manufacture

ABSTRACT

New structural efficiency diagrams are presented for laminates, showing that additional mass is incurred when (i) laminate balancing axes are not aligned with principal loading axes and (ii) principal loading ratios vary within a part with fixed ply percentages. This presents an opportunity for fibre steering and laminate tailoring in aerospace design. Non-standard ply angles are shown to offer small mass savings when laminate balancing axes are not aligned with principal loading axes. However, such angles may enhance performance in other aspects (e.g. damage tolerance, ease of manufacture, buckling resistance) whilst matching the in-plane stiffness of standard ply angle designs.

1 INTRODUCTION

Netting analysis [1], in which fibres only carry load in their longitudinal direction with the resin matrix ignored, indicates that designs with fewer than three fibre directions produce mechanisms when subject to small disturbances in loading. This reveals the robustness of established aerospace laminate design practice which uses four standard angles (0º, +45º, -45º and 90º) to provide a level of redundancy in load carrying whilst allowing for the manufacturing requirement of balanced angle plies. Laminates for aerospace components are currently designed using standard ply angles whilst following established design rules [2]. These rules include: ply angle symmetry about the laminate mid-plane, equal numbers (balancing) of +45º and -45º angle plies, 10% thickness in each of the 4 ply angles, and ply blocks of identical angles must be a maximum of 1mm. Additionally, ±45º plies are usually positioned at the outer surface for enhanced damage tolerance. The percentage of 0º/±45º/90º plies in a laminate is a function of the typical loading a component will carry; for example in wing skins, stiffeners and wing spars, target percentages are typically 44/44/12, 60/30/10 and 10/80/10, respectively. Unfortunately, such rules can restrict laminate designs whilst satisfying the required curvature-stable manufacturability and stiffness coupling constraints [3, 4]. And so the potential for non-standard plies to improve in-plane performance is explored in this paper.

Clearly, any shift in design practice toward non-standard angles cannot come at the cost of laminate performance, where laminate tailoring and tow-steering are pushing the boundaries of minimum mass composite structural design [5]. Efforts are also being made to make the composite laminate design process simpler and more accessible [6]. Thus, in combination with a method for finding non-standard ply angles that match the in-plane stiffness of standard ply angles, a simple strain energy (compliance) minimisation is used to compare performance of standard and non-standard laminates. Minimisation of elastic strain energy allows laminates to be designed that store the least energy, creating the stiffest configuration for a given design loading. Prager and Taylor [7] first outlined optimality criteria justifying the technique of minimisation of elastic energy to produce a structure with optimal efficiency. Pedersen [8] subsequently applied this technique to composite materials to find analytical solutions for orientation of a single ply angle subject to in-plane loading. This is a logical design concept as the material is made to work as hard as possible to resist deformation under load, and thus is efficiently used, potentially allowing lower mass designs to be produced. However, such design does not directly convert to minimum mass, as failure is nonlinear and complex; comprising damage to both resin and fibre, which is induced by mechanisms such as delamination, buckling, bearing, edge effects and manufacturing defects. Nevertheless, in this paper elastic energy is considered to be an indication of

performance to assess the potential of different design approaches to reduce laminate mass. Further to the above, manufacturing constraints mean that lay-up axes and principal loading axes are not necessarily aligned. Hence results are presented to illustrate the effect of aligning (and misaligning) the laminate balancing axes with the principal loading axes.

2 THEORY

The following outlines the theory required (i) to create non-standard ply laminates with matching in-plane stiffness to standard ply laminates and (ii) to assess the comparative performance of standard and non-standard ply laminates, where performance is quantified by elastic energy.

2.1 Equivalent representation of laminate stiffness

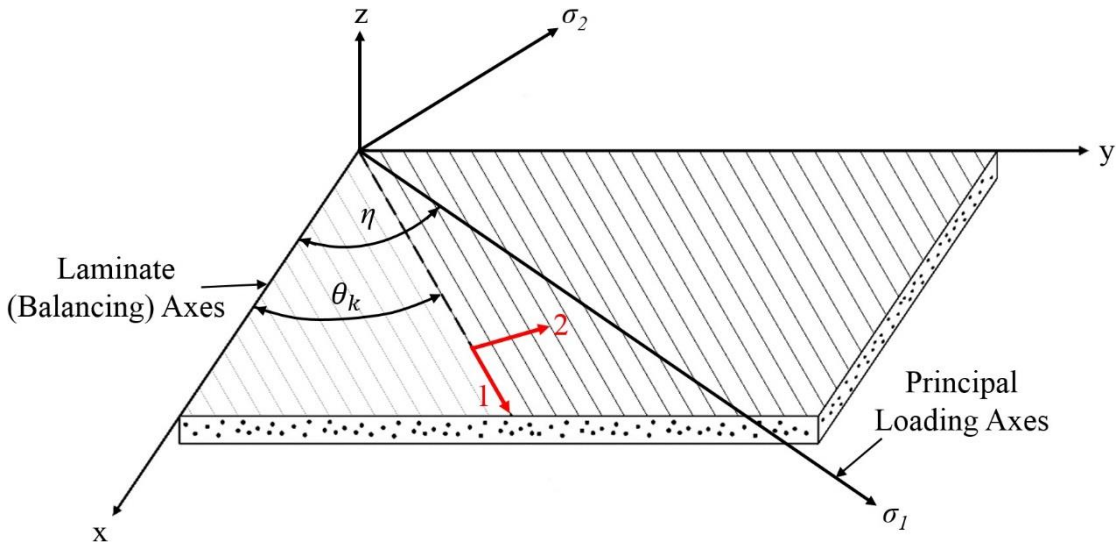

Fig. 1. Local ply axes (1-2) and laminate (balancing) axes (x-y-z). The principal loading axes and misalignment angle η from the balancing axes are also shown.

Assuming that (i) the laminate is balanced with zero in-plane to out-of-plane coupling (i.e. Q_{16}, Q_{26} = 0) and (ii) a state of plane stress ($\sigma_z, \tau_{xz}, \tau_{yz} = 0$), exists. Classical Laminate Theory gives the in-plane laminate stress-strain relationship as

$$\{\sigma\} = \begin{Bmatrix} \sigma_x \\ \sigma_y \\ \tau_{xy} \end{Bmatrix} = \{N\}/T = \frac{1}{T}\begin{Bmatrix} N_x \\ N_y \\ N_{xy} \end{Bmatrix} = [Q]\{\varepsilon\} = \begin{bmatrix} Q_{11} & Q_{12} & 0 \\ Q_{12} & Q_{22} & 0 \\ 0 & 0 & Q_{66} \end{bmatrix}\begin{Bmatrix} \varepsilon_x \\ \varepsilon_y \\ \gamma_{xy} \end{Bmatrix} \tag{1}$$

where subscripts *x* and *y* refer to laminate axes in Fig. 1 and σ_x, σ_y, τ_{xy} (and ε_x, ε_y, γ_{xy}) are the applied in-plane axial, transverse and shear stresses (and corresponding laminate strains), respectively. The Q_{ij} terms represent the individual in-plane stiffnesses and can be defined using lamination parameters and stiffness invariants [9-12].

2.2 Equivalent stiffness of laminates with standard and non-standard ply angles

Lamination parameters are plotted in Fig. 2 to demonstrate the relative extent of design spaces for laminates made of (i) standard angle plies and (ii) two balanced non-standard angles $(\pm\psi)_\gamma/(\pm\phi)_{1-\gamma}$. Note that γ defines the proportion of $\pm\psi$ plies and standard angle designs are seen to be a subset of the non-standard angle ply design space [10-12]. The procedure for stiffness matching of standard angles with balanced non-standard angles, $(\pm\psi)_\gamma/(\pm\phi)_{1-\gamma}$, using lamination parameters is outlined below,

with the general ply axes outlined in Fig. 1. The ξ_1 and ξ_2 lamination parameter terms can be defined using the individual in-plane stiffnesses (Q_{ij}) and stiffness invariants U_{1-5} [12-14].

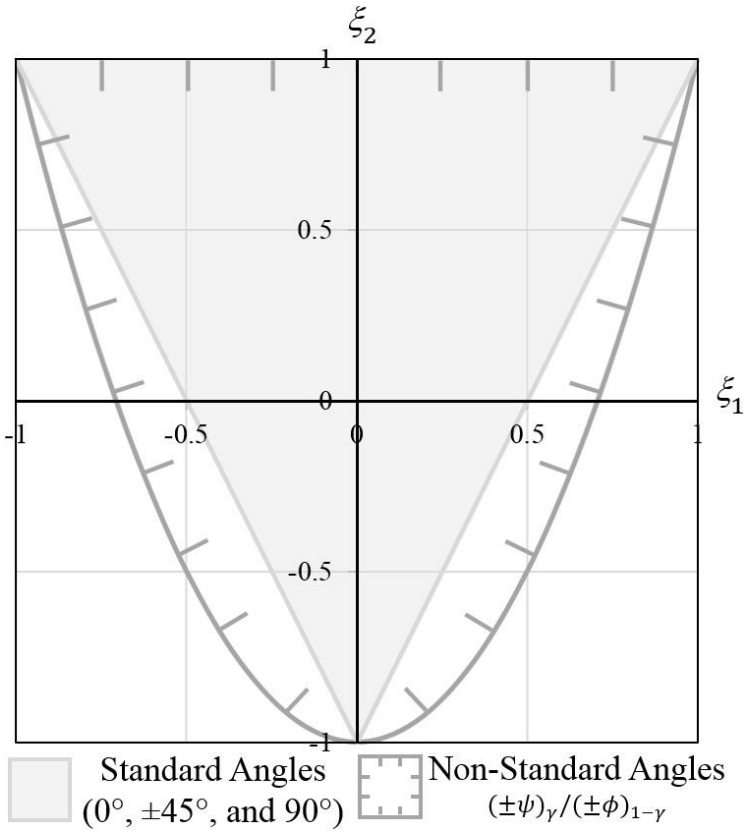

Fig. 2. Comparison of in-plane lamination parameter design space for standard and non-standard angle $(\pm\psi)_\gamma/(\pm\phi)_{1-\gamma}$ laminates with ply percentage variation permitted. The standard angle design space is a subset of the non-standard angle space.

Assuming a given set of values for a standard angle laminate Q_{ij}^S, (where superscript S indicates standard plies) values of in-plane lamination parameters are sort that reproduce Q_{ij}^S using non-standard angles. Full derivation is shown in Nielsen et al. [11].

$$\xi_1 = \frac{Q_{11}^S - Q_{22}^S + Q_{12}^S - Q_{66}^S - U_4 + U_5}{2U_2} \tag{2}$$

Hence, from Eq. (2), any given proportion of standard angles within a laminate will have a certain value of ξ_1. In order to represent ξ_1 by two balanced non-standard angles $\pm\psi$ and $\pm\phi$ of proportion γ and $1-\gamma$, respectively, we define the following parameters

$$\left.\begin{aligned} \alpha &= \cos 2\psi \qquad & -1 < \alpha < 1 \\ \beta &= \cos 2\phi \qquad & -1 < \beta < 1 \end{aligned}\right\} \tag{3}$$

Since

$$\xi_1 = \frac{1}{T}\int_0^T \cos 2\theta_k \; dz = \frac{1}{T}\sum_{k=1}^{m} \cos 2\theta_k t_k \tag{4}$$

$$\xi_2 = \frac{1}{T}\int_0^T \cos 4\,\theta_k \; dz = \frac{1}{T}\sum_{k=1}^{m} \cos 4\theta_k t_k \tag{5}$$

Therefore from Eq. (3) and Eq. (4) we obtain,

$$\xi_1^N = \gamma\alpha + (1-\gamma)\beta \tag{6}$$

where ξ_1^N and ξ_2^N are lamination parameters for non-standard angle layups. Hence

$$\gamma = \frac{\xi_1^N - \beta}{\alpha - \beta} \tag{7}$$

The relationship below is known

$$\xi_2 = \frac{U_5 - Q_{66}^S}{U_3} \tag{8}$$

As before, any given standard laminate will also have a certain value of $\xi_2$creating a unique pair of values ξ_1 and ξ_2. Applying a similar process as Eqs. (3) and (6), by making the double angle substitution, gives

$$\xi_2^N = \gamma(2\alpha^2 - 1) + (1-\gamma)(2\beta^2 - 1) \tag{9}$$

Now rearranging and solving for β and substituting for γ from Eq. (7) we have

$$\beta = -\left(\frac{\xi_2^N + 1 - 2\alpha^2}{4(\alpha - \xi_1^N)}\right) \pm \sqrt{\left(\frac{\xi_2^N + 1 - 2\alpha^2}{4(\alpha - \xi_1^N)}\right)^2 - \left(\frac{2\alpha^2\xi_1^N - \alpha - \xi_2^N\alpha}{2(\alpha - \xi_1^N)}\right)} \tag{10}$$

If we choose any angle $\pm\psi$ and hence its corresponding value of α from Eq. (3), we can use Eqs. (2), (8) and (10) to define β, which can then be used to obtain the second angle $\pm\phi$. The thickness proportion of these two sets of angles is then given by Eq. (7). A given standard angled laminate can therefore be fully matched by repeating this process for all values of $\pm\psi$, provided that solutions to Eq. (10) are in the range $-1 \leq \beta \leq 1$.

2.3 Laminate elastic energy

The expression for normalised elastic energy per unit volume is shown in Eq. (11), representing the effective laminate compliance that is independent of load magnitude and laminate thickness. A lower value corresponds to a higher global laminate stiffness and more efficient use of material. Derivation included in Nielsen et al [11].

$$\bar{U}_V = \frac{q_{11}\sigma_x^2 + 2q_{12}\sigma_x\sigma_y + q_{22}\sigma_y^2 + q_{66}\tau_{xy}^2}{2(\sigma_1^2 + \sigma_2^2)} \tag{11}$$

Where

$$\boldsymbol{\sigma_{1,2}} = \frac{\boldsymbol{\sigma_x} + \boldsymbol{\sigma_y}}{\mathbf{2}} \pm \sqrt{\left(\frac{\boldsymbol{\sigma_x} - \boldsymbol{\sigma_y}}{\mathbf{2}}\right)^{\mathbf{2}} + \boldsymbol{\tau_{xy}^2}} \tag{12}$$

Substitution of Eq. (12) into Eq. (11) gives

$$\bar{U}_V = \frac{q_{11}\sigma_x^2 + 2q_{12}\sigma_x\sigma_y + q_{22}\sigma_y^2 + q_{66}\tau_{xy}^2}{2\left(\sigma_x^2 + \sigma_y^2 + 2\tau_{xy}^2\right)} \tag{13}$$

3 STACKING SEQUENCE OPTIMISATION FOR MINIMUM ELASTIC ENERGY

The performance of a laminate subject to a multi-axial state of stress is assumed to be represented by its Hookean strain energy or elastic energy; minimum energy indicates maximum performance. For each design loading, a Matlab genetic algorithm (GA) function '*ga*' [13] finds the laminate design that minimises the laminate elastic strain energy in Eq. (13) thus creating designs with $\bar{U}_{V,min}$. GA optimisation is halted if either the maximum number of iterations reached 5000 or if the change in the elastic energy value between iterations was less than $1\text{x}10^{-20}$ m^2/N.

Optimisation of both standard (0°, ±45°, and 90°) and non-standard angle $((\pm\psi)_\gamma/(\pm\phi)_{1-\gamma})$ laminates was performed by the GA. The ply percentage for each angle was allowed to vary continuously. Non-Standard angles were set to vary at integer values in the range 0° to 180°. Standard angle results were produced both with and without a 10% design rule in which a minimum of 10% of each of the four ply angles is maintained. This rule is enforced by limiting the choice of ply percentages available to the GA.

Standard angle laminates are normally restricted to a fixed coordinate system about which laminates are balanced (for example, the 0° fibres are aligned from root to tip in a wing skin) [2]. In both standard and non-standard laminates, an equal number of positive and negative angle plies ensures all designs are balanced about the 0° laminate axes unless otherwise stated, see Fig. 1. All general load states in the laminate (balancing) axes can be described by their principal loading and a misalignment angle, η, from the balancing axes, shown in Fig. 1. η = 0° is a special case where the principal loading axes are aligned with the balancing axes. This is generally not the case in design as the balancing axes are aligned with the laminate manufacturing axes. However, balance could potentially be achieved in different axes, thereby enforcing η = 0°. In the results that follow a spread of 136 principal loading ratios, σ_1/σ_2, are considered. Each principal load ratio is applied with a range of different misalignments, η, where η is varied in increments of π/128 from 0 to π giving a total of 17,408 designs.

4 RESULTS

4.1 Standard and non-standard laminates with equivalent in-plane stiffness

Laminates for stiffener, skin and spar wing components typically have standard angle (0°/±45°/90°) ply percentages of 60/30/10, 44/44/12 and 10/80/10 respectively. For each application Figs. 3(a) and (b) show a matched stiffness design space for non-standard angles derived from the equations of Section 2.2. Note that, in order to satisfy the requirement of generating a [*Q*] identical to the original standard

angle laminate, both values for the thickness proportion γ and angle ϕ vary with a change in initial angle ψ. Highlighted points in Fig. 3 represent an arbitrary example for the spar laminate, where angle ψ is set at ±31.7° and the second angle ϕ = ±58.3° is derived from Eqs. (3), (7) and (10). The thickness proportion $\gamma = 0.5$, indicates a 50/50 distribution of angle sets.

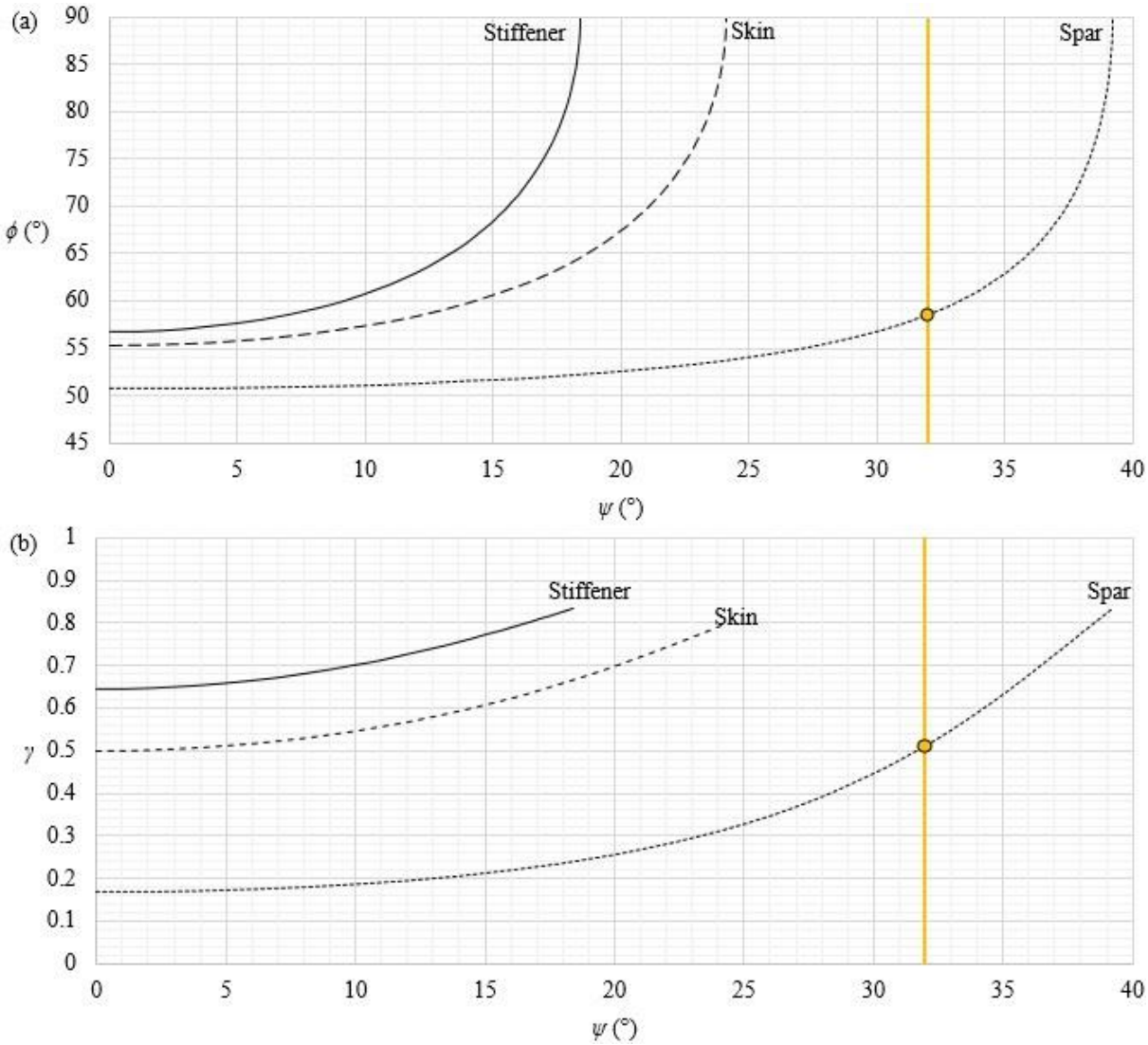

Fig. 3. (a) Non-standard ply angles $(\pm\psi)_\gamma/(\pm\phi)_{1-\gamma}$ for laminates with equivalent in-plane stiffness of standard angle stiffener (60/30/10), skin (44/44/12) and spar (10/80/10) laminates. (b) Contribution (γ) to laminate thickness of ply angle pair $\pm\psi$.

4.2 Performance optimisation

Results in Fig. 4 were obtained using the procedure in Section 3 and describe variation in minimum elastic energy with principal design load for both optimised standard angle (with and without the 10% rule) and non-standard angle designs. Radial variation indicates the magntiude of elastic energy. Angular variation specifies the ratio of principal loading σ_1/σ_2. The inner and outer limits (rings) of Fig. 4 indicate limits on the minimum elastic energy $\overline{U}_{V,min}$ with variation in η, the prinicpal loading to balancing axes misalignment. Inner rings show the lowest (best) achievable minimum elastic energy from variation in η. This occurs for η = 0° where the principal loading axes is aligned with the balancing axes. Outer rings show the upper bound of minimum elastic energy with variation in η. Laminate designs represented by

the outer ring are optimised for minimum (best) energy whilst meeting the constraint of worst possible misalignment η_w i.e. non-optimised laminate designs may have energies that sit outside the outer ring. All optimised minimum elastic energy $\bar{U}_{V,min}$ results, for all values η, lie between the inner and outer rings. Note that non-zero misalignment indicates the optimised design is under both shear and direct load.

Design Point	% 0°	% ±45°	% 90°	Design Load		Applied Load		$\bar{U}_V$ (x10^{-12} m^2/N)	Equivalent Mass: $\sqrt{\bar{U}_V}$ (% Increase at Cap)
				σ_1/σ_2	η (°)	σ_1/σ_2	η (°)		
A1	50.0	0.0	50.0	-1 (W)	0	-1 (W)	0	7.5	2.7
A1*	50.0	0.0	50.0	-1 (W)	0	-3 (C)	15	27.9	5.3 (+31%)
A2	40.0	20.0	40.0	-1 (W)	0	-1 (W)	0	9.0	3
B1	40.0	20.0	40.0	-1 (W)	0	-3 (C)	15	16.3	4 (datum)
B2	58.9	30.7	10.4	-3 (C)	15	-3 (C)	15	9.5	3.1 (-24%)
B3	78.1	0.0	21.9	-3 (C)	0	-3 (C)	0	6.0	2.5 (-39%)

Table 1 Laminate designs, design loads and applied loads in spar web (W) and spar cap (C) for Points A1-B3, shown in Fig. 4. Note that design Point A1* is not shown in Fig. 4.

A spar design case is used to illustrate the effect of the misalignment angle η. Pure shear load may be expected near the centre of a spar web corresponding to, σ_1/σ_2 = -1 at 45° to pure shear, see Fig. 5. The design represented by point A1 in Fig. 4, consisting of 50% of 0° plies and 50% of 90° plies (i.e., ±45° plies in pure shear), is the optimal laminate for this loading for both standard and non-standard angles. Point A2 in Fig. 4 corresponds to the equivalent standard angle laminate design problem but with the 10% minimum ply percentage rule enforced. However, loading varies across the spar and a different design will be optimal at the spar caps where bending stresses are significant and $\sigma_1/\sigma_2 \neq -1$, see Fig. 5. If the same magnitude of shear that occurs in the web is assumed to occur in the spar caps and assuming σ_1/σ_2 = -3, then from Mohr's circle, see Fig. 5(a), a tri-axial load state of σ_x/σ_y = -3.73 and σ_x/τ_{xy} = 2.73 is created in the spar axes where η = 15º. Point B1, in Fig. 4 and Table 1, and Point A1* (in Table 1 only) indicate the energies achieved if this spar cap loading is applied to the designs for Points A2 and A1, respectively. This represents inferior performance at the spar cap if current manufacturing practice is followed and web laminate designs are maintained throughout the spar.

Points B2 and B3 represent minimum elastic energy for standard angle laminates optimised for the cap loading whilst balancing in the spar (η = 15º) and principal axes (η = 0º), respectively.

Variation in ply percentages of optimum standard angle designs with principal load ratio, corresponding to the energy of inner and outer rings of Fig. 4, is shown in Fig. 6(a) and (b), respectively. Figure 6(a) shows that if axial (transverse) loading dominates, there are a larger proportion of 0° (90°) plies. The requirement for ±45° plies is seen to only exist for positive principal load ratios. However, optimum designs corresponding to the outer ring in Fig. 6(b), where the principal loading is not aligned with the balancing axes, require a combination of 0°, ±45° and 90° plies.

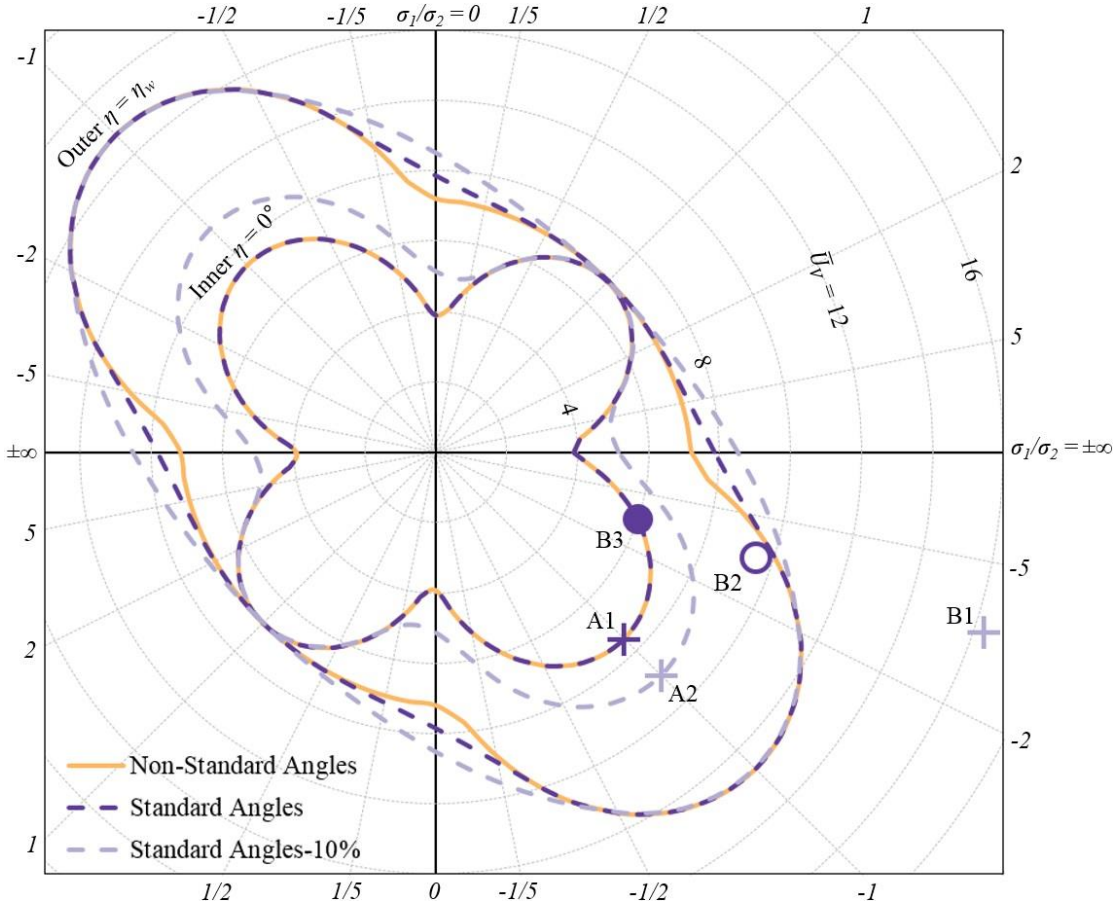

Fig. 4. Comparison of elastic energy $\overline{U}_V$ (x10^{-12} m^2/N) for optimised standard angle laminates (with and without the 10% rule) and non-standard angle laminates designed for radially varying principal load ratios σ_1/σ_2. The inner and outer rings represent, respectively, the best and worst misalignment, η, of the principal loading with the balancing axes. Points A1-B3 refer to specific designs in Table 1.

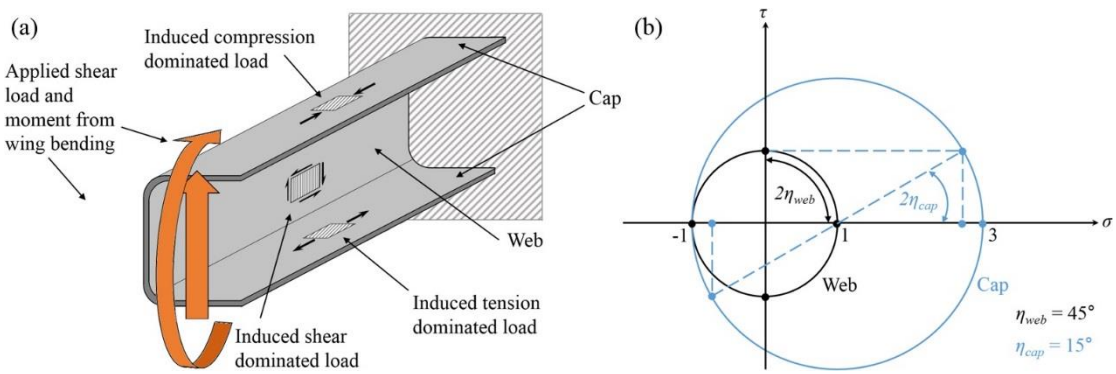

Fig. 5. (a) Schematic view of idealised loading of a spar section. Web and cap sections together with dominant loading type are identified. (b) Mohr's circle representation of the example spar web and spar cap loadings of σ_1/σ_2 = -1 (at 45° to pure shear) and σ_1/σ_2 = -3 at η = 15°, respectively, for the loading applied to design Points A and B in Table 1 and Fig. 4.

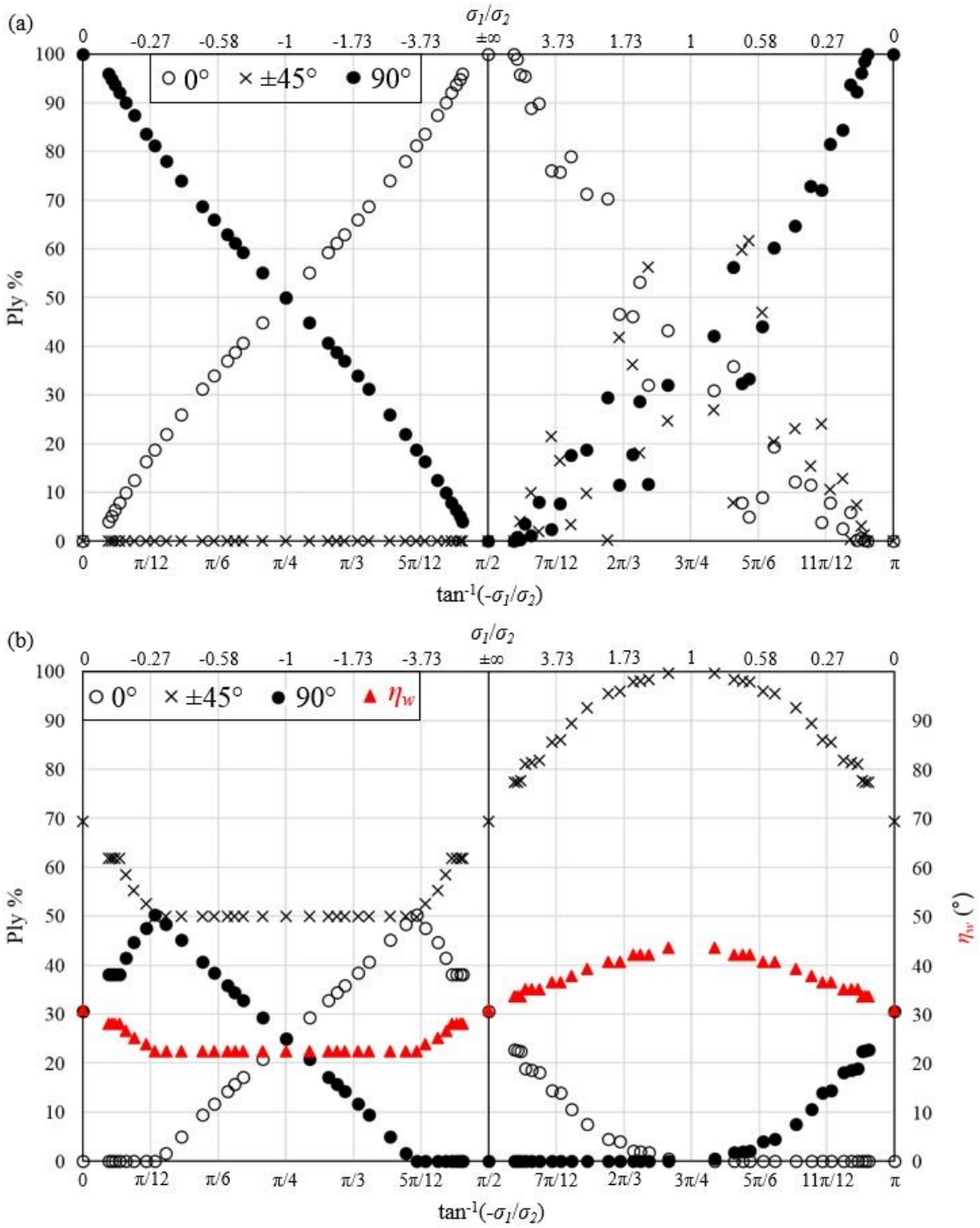

Fig. 6. Ply percentage variation of the optimum standard angle laminate designs for (a) the Fig. 3 inner ring and (b) the outer ring. The η_w shown in (b) corresponds to the worst case misalignment of the principal loading to balancing axes. Note designs are not presented for the special case of $\sigma_1/\sigma_2 = 1$ (hydrostatic pressure) but are described in Section 5.2.

5 DISCUSSION

5.1 Standard and non-standard laminates with equivalent in-plane stiffness

Figure 3 shows that stiffness matching of standard angle laminates with non-standard angle laminates can be achieved over a range of non-standard angles. While maintaining the exact stiffness properties of the original standard angle laminate, non-standard angles can be freely chosen to satisfy design

requirements for improved manufacturability or laminate performance such as buckling resistance or damage tolerance. The three design examples explored in Fig. 3 carry very different loadings which limit the range of non-standard matched stiffness designs to a greater or lesser extent. The standard stiffener laminate, which has the highest proportion of 0° fibres, offers the smallest range of ψ that can be paired with ϕ angles to generate a $[Q]$ identical to the original standard laminate. In contrast, the standard spar laminate which is dominated by ±45° plies, allows for twice the range in angle ψ. Similarly, this contrast in range applies for the thickness proportion γ.

It is noted that, despite having very different fibre proportions, all three design cases produce a non-standard fibre angle combination where ϕ always takes a value between 50° and 90°. The stiffener and skin laminates also produce a very similar angle for ϕ in the low regions of ψ. This creates the potential for a composite structure that has areas with different performance criteria, to incorporate one common ply angle. The common transition method between two areas, ply dropping, would therefore result in a much more uniform changeover in material properties.

5.2 Optimisation for performance

Principal load ratio inherently affects the value of minimum elastic energy possible as seen by the variation in magnitude around the inner ring in Fig. 4. In Table 1, Points A1 and B3 show that to create the lowest achievable minimum elastic energies for the inner ring in Fig. 4, the principal load must be aligned with the balancing axes ($\eta = 0°$). However, it is uncommon for a principal loading to be aligned with the balancing axes. Therefore, realistically achievable energies will lie above the inner rings as there is an increase in the elastic energy stored due to extra shear deformation from the presence of a shear load when $\eta \neq 0°$.

No designs are plotted for $\sigma_1/\sigma_2 = 1$ in Figs. 6(a) and (b) as there are many optimum designs where any rotation of any combination of a π/n quasi-isotropic (QI) laminate (where n is an integer ≥ 2) is optimal.

Principal loading is essentially bi-axial if balancing in the principal axes is allowed ($\eta = 0°$) or if the principal load is already aligned to the laminate axes, which is an unlikely design scenario. Under such conditions, non-standard angle plies offer no elastic energy advantage over standard angle plies, even though the designs are potentially different, see inner rings in Fig. 6. The optimal laminate stiffness requirements for bi-axial design loads must then lie within the standard angle lamination parameter design space shown in Fig. 2 [10-12]. It is only when a tri-axial design load exists ($\eta \neq 0°$), equivalent to a misaligned principal loading to the balancing axes, which is often the case in practical design, that an advantage appears for use of non-standard plies, as seen by the difference in elastic energy of the outer rings in the vicinity of $\sigma_1/\sigma_2 = \pm\infty$ and $\sigma_1/\sigma_2 = 0$.

Figure 4 shows that application of the 10% minimum ply percentage rule generally increases the minimum elastic energy achievable. This is especially true where entirely 0º or 90º designs are theoretically optimal, and for all compressive-tensile principal loadings ($-\infty < \sigma_1/\sigma_2 < 0$), where optimal designs require a combination of 0º and 90º plies and no ±45º plies. However, the 10% rule creates robustness to variation in loading. For example, under the web design load of pure shear there is a small energy penalty at Point A2 compared to Point A1 but when applying the spar cap loading, the elastic energy is significantly less, see Point B1 compared to A1* in Table 1. The 10% rule is, however, arbitrary and is not required for a deterministic loading condition. Point B2, which has a potential 24% reduction in mass over Point B1, is a realistic optimal design if the spar cap loading is assumed to be fixed and known, but also satisfies the 10% rule and represents the optimum design with the rule enforced, allowing robustness to load uncertainty. Going from the design Point A2 to Point B2 shows the potential to modify laminate ply percentages from a spar web to cap to account for variation in load ratios. If the 10% rule and the requirement to balance in the spar/laminate axes are also removed, further improvement is seen at Point B3 with a 39% potential mass reduction over Point B1, highlighting the

potential benefit of steering fibres throughout the part from Point A1 at the web. Balancing in the principal axes is more worthwhile for $-\infty < \sigma_1/\sigma_2 < 0$, where the addition of shear from the misalignment creates higher mass designs, shown by higher energies in the outer ring designs compared to $\infty > \sigma_1/\sigma_2 > 0$, where greater proportions of ±45º plies are required.

In Fig. 6 the optimum designs corresponding to the inner rings are unique for $\sigma_1/\sigma_2 \leq 0$ and $\sigma_1/\sigma_2 = \pm\infty$ when $\eta = 0º$. This is because 0º and 90º plies are able to provide optimal stiffness properties. A smooth variation in 0º and 90º ply percentage is seen in Fig. 6(a) over these loadings adding evidence that no other optimal laminates are possible. However for $0 < \sigma_1/\sigma_2 < \infty$ optimal designs are not unique as shown in the scattered distribution of the standard angle ply percentages in Fig. 6(a). This suggests that different optimal [*Q*] matrices exist for the same design loading, and is confirmed by the presence of different optimal [*Q*] matrices in the optimised non-standard angle laminates that provide identical minimum energies.

In summary, minimum elastic energy is seen to be limited by (i) the principal loading ratio, (ii) the 10% ply percentage rule and (iii) the principal loading axes misalignment with the balancing axes, η. If the loading is known to be fixed and/or there is no requirement to balance in a fixed axes, then there is potential to design lower mass laminates.

6 CONCLUSIONS

Elastic energy minimisation is applied to improve performance through the use of non-standard ply laminate designs and balancing of plies about an axes with variable misalignment from principal loading axes.

The performance of a laminated composite aircraft component, ignoring complex failures such as kink banding, buckling and compression after impact, is dependent on orientating plies such that load is carried predominantly by the fibres. The capacity of a laminate stacking sequence to direct a multi-axial in-plane load into the stiffer fibres can be measured by assessing its elastic energy under a specific design load. It was found that laminate designs for optimal performance occur when balancing axes are fully aligned with principal loading axes. In this case, use of non-standard plies is shown to have no benefit; for positive biaxial loading ratios the design space available was significantly enlarged as multiple combinations of non-standard plies were available to match standard angle laminate stiffness. Some performance benefit was found from non-standard angles when, as is often the case in aerospace components, the balancing axes is misaligned from the principal loading axes. Non-standard angle plies whilst matching in-plane performance can potentially become more useful for other design objectives, such as damage tolerance, manufacturability and buckling resistance. Example aerospace component loading scenarios demonstrated that if principal load axes vary across a component (e.g. web to cap in a spar) then significant benefit could be derived from stiffness tailoring through tapering and tow-steering.

ACKNOWLEDGEMENTS

We are grateful for the input of Dr Richard Newley. Richard Butler holds a Royal Academy of Engineering/GKN Research Chair.

REFERENCES

[1] G. Verchery, The Netting analysis as a limit case of the laminated structure theory, *Proceedings of the 19th International Conference on Composite Materials (Eds. S.V. Hoa, P. Hubert), Montreal, Canada, July 28-August 2, 2013,* Canadian Association for Composite Structures and Materials (CACSMA), Montreal, 2013, pp. 1724-1731

[2] M.C.Y. Niu, *Advanced composite structures*, Airframe structural design - Practical design information and data on aircraft structures (2nd edition), Conmilit Press Limited, Hong Kong, 1999.

[3] S.J. Winckler, Hygrothermally curvature stable laminates with tension-torsion coupling, *Journal of the American Helicopter Society*, **30**, 1985, pp. 56-58.

[4] C.B. York, Tapered hygro-thermally curvature-stable laminates with non-standard ply orientations, *Composites Part A: Applied Science and Manufacturing*, **44**, 2013, pp. 140-148.

[5] Z. Gurdal, B. Tatting and C. Wu, Variable stiffness composite panels: Effects of stiffness variation on the in-plane and buckling response. *Composites Part A: Applied Science and Manufacturing*, **39**, 2008, pp. 911–922.

[6] S.W. Tsai and J.D.D. Melo, An invariant-based theory of composites. *Composites Science and Technology*, **100**, 2014, pp. 237–243.

[7] W. Prager and J.E. Taylor, Problems of optimal structural design, *Journal of Applied Mechanics*, **35**, 1968, pp. 102-106.

[8] P. Pedersen, On optimal orientation of orthotropic materials, *Structural Optimization*, **1**, 1989, pp. 101-106.

[9] S.W. Tsai and N.J. Pagano, *Invariant properties of composite materials*, Composite materials workshop, Technomic Publishing Company, St. Louis, Missouri, 1968.

[10] M. Miki and Y. Sugiyama, Optimum design of laminated composite plates using lamination parameters, *AIAA Journal*, **31**, 1993, pp. 921-922.

[11] M. Nielsen, K.J. Johnson, A.T. Rhead and R. Butler, Laminate design for optimised in-plane performance and ease of manufacture, *Composite Structures* (submitted: Nov. 2016).

[12] C.G. Diaconu and H. Sekine, Layup optimization for buckling of laminated composite shells with restricted layer angles, *AIAA Journal*, **42**, 2004, pp. 2153-2163.

[13] MATLAB R2013b, MathWorks, 2013, Natick, Massachusetts.